Pressure dependence of the contact angle in a CO_2-H_2O-coal system

Nikolai Siemons Hans Bruining Hein Castelijns
Karl-Heinz Wolf
Dietz Laboratory, Centre of Technical Geoscience
Mijnbouwstraat 120
2628 RX Delft, The Netherlands

March 22, 2005

Abstract

Carbon dioxide injection into coal layers serves the dual purpose to enhance coal bed methane production (ECBM) and CO_2 storage. The efficiency of this process is expected to be much higher if water is the non-wetting phase in the coal-water-gas system. Therefore the contact angle in the coal-water-CO_2 system has been measured using the captive bubble technique in the pressure range between atmospheric and 141 bar at a temperature of 45^oC. At atmospheric pressures the contact angle of a shrinking CO_2 droplet increases with time, but stays below 90^o, At higher pressures (> 2.6 bar) the contact angle increases beyond 90^o. The contact angle increases with increasing pressure and can be represented by $\theta = (111^o \pm 10.5^o) \pm (0.17 \pm 0.14)\, P\,[bar]$. The exceptional behaviour at atmospheric pressure is possibly related to the stability of water patches on the coal surface. It is concluded that water is the non-wetting phase in this the coal-water-CO_2 system.

Keywords: wetting properties, water-CO_2-coal system, high pressure, contact angle

1 Introduction

One of the promising methods to reduce the discharge of the "greenhouse gas" carbon dioxide (CO_2) into the atmosphere is its sequestration in unminable coal seams. A typical procedure is the injection of carbon dioxide via deviated wells drilled inside the coal seams. Carbon dioxide displaces methane (CH_4) adsorbed on the internal surface of the coal. A production well gathers the methane as free gas. This process, known as carbon dioxide-enhanced coal bed methane production (CO_2-ECBM), is a producer of natural gas and at the same time reduces greenhouse gas emissions as two carbon dioxide molecules displace

one molecule of methane. Coal has an extensive fracturing system called the cleat system. In actual fact it is possible to discern a number of cleat systems at different scales. The matrix blocks between the smallest cleat system have diameters typically of a few tens of microns [7]. After an extensive dewatering phase, carbon dioxide is injected and flows mainly through the larger cleats of the coal. From there it diffuses through the smaller cleats and subsequently adsorbs in the matrix blocks.

Consequently, before CO_2 can reach the coal matrix containing the methane it must first diffuse through a network of smaller cleats. If the cleat system is filled with water, the diffusion rate is small ($D \approx 2 \times 10^{-9} m^2/s$). If the cleat system is filled with gas the diffusion rate is much larger i.e. $D \approx 1.7 \times 10^{-7} m^2/s$ at 100 bar [2]. It is expected that the smaller cleat network is filled with water if the coal-water-gas system is water-wet and filled with gas if water is the non-wetting phase. We therefore assert that the wetting behavior plays an important role in CO_2-ECBM production. For this reason we have undertaken an experimental study of the wetting behavior of a coal-water-CO_2 system as a function of pressure.

Contact angle measurements provide a simple method to characterize the interfacial energies of a solid in contact with fluids and thus the wetting behavior [1]. Very often, these measurements are performed by direct observations of drops deposited on the solid, and viewed from the side. Overview articles describe in detail various technical aspects of a set-up that measures droplet shapes [18].

Investigations of the wettability behavior of coal reported in the literature are largely based on contact angle measurements for the coal-water-air system at atmospheric pressure. Gutierrez et al. [8] found that the contact angle depends on the coal rank. They [9] also quantified the effect of surface oxidation using the captive bubble technique. In general, three types of surface components can be distinguished i.e. strongly hydrophobic, weakly hydrophobic and hydrophilic. Low rank coals appear to be hydrophilic and coals become increasingly hydrophobic with increasing rank. Murata [17] performed measurements on pressed pellets of pulverized coal. It is found that the contact angle depends on the hydrogen and oxygen content of the coal. Keller [15] has summarized literature data [8], [9], [5], [17] on the coal-water-air system. The contact angles appear to be largely in the range between $60^o - 90^o$. Keller [15] is able to represent observed trends in measurements of the contact angle θ by assuming that $\cos\theta$ is an area weighted average of the cosine of the contact angles on the heterogeneous surface. To our knowledge there are no contact angle measurements of coal at elevated pressures.

The usual problems with contact angle measurements are all encountered with contact angle measurements on coal. First, surface oxidation alters the properties of the coal surface. Gutierrez-Rodriguez et al. [8] , [9] observed a contact angle decrease (increased hydrophilic behavior) in a water-air coal system after exposing its surface for several hours to oxygen sparged water. Secondly, the wettability of the coal surface is strongly heterogeneous due to its heterogeneous composition. Keller [15] found strongly hydrophobic behavior

for the paraffinic hydrocarbon fraction, intermediate behavior for the aromatic fraction and strongly water wet behavior for the minerals and water filled pores. The wettability heterogeneity leads to a varying contact angle. Consequently the droplet will have a non-spherical shape and a non-circular three phase contact line. As a result the left and right contact angles observed in a vertical cross-section will be slightly different. However, large variations of contact angles along the three phase contact line lead to a large water-gas interface, which is energetically unfavorable. Therefore the equilibrium droplet shape favours smooth variations along the three phase contact line. This also explains the empirical equation proposed by Keller [15] i.e. the cosine of the contact angle equals a weighted average of the cosines of the contact angles of the components constituting the coal surface.

The determination of the contact angle puts severe demands on the smoothness of the surface [6], [4], [18]. The contact angle hysteresis i.e. the difference between the advancing and receding angle may be 10^o or more for non-smooth surfaces. Joanny and de Gennes [14] point out that the main reasons for contact angle hysteresis are the surface energy fluctuations related to rough surfaces and chemical heterogeneity. Rough parts of the surface are partially smoothed because the wetting fluid fills the crevices leading to composite surfaces consisting of substrate and the wetting fluid. The same phenomenon is also expected to remove roughness on a very small scale. De Gennes [6] relates the force exerted by the surface heterogeneity on the contact line to the force originating from the distortion of the interface on the contact line. The latter is described as an elastic force proportional to the deviation of the position of the contact line with respect to its unperturbed position. When the surface energy heterogeneity is small there is only one solution and there is no contact angle hysteresis. When the surface energy heterogeneity is sufficiently large there is more than one stable solution and hysteresis is expected. From the analysis it is clear that the solid surface must be smooth. Drelich et al. [3] state that in practice reproducible contact angles on coal can be obtained if the micro-roughness of the coal surface i.e. the height distance between tops and valleys is less than $40 - 55nm$. Equilibrium contact angles get established after all three phases get in contact with each other.

A number of electrochemical processes are relevant. A water film formed on the coal surface must be ruptured [10], [11], [12] before contact between the carbon dioxide and the coal surface is established. As a result an equilibrium contact angle will only be established after some time. In addition, two aspects that are specific for the coal-carbon dioxide-water system are important. Contact angles between coal and carbon dioxide are expected to be influenced by the adsorption of CO_2 on the surface. According to Gibbs' equation, the surface tension between water and coal decreases due to adsorption on the surface. This would lead to a contact angle increase. Furthermore to avoid random formation of CO_2 droplets we did not saturate the water with carbon dioxide at the prevailing pressure. As a consequence, however, diffusion of CO_2 into the water phase will occur and the droplet will decrease in size. From the view point of the CO_2 droplet we observe two receding contact angles at the left and right

side of the droplet.

Considering all of this it is clear that useful information regarding wetting behavior can be extracted from contact angle measurements provided that due attention is given to make the surface sufficiently smooth to obtain reproducible results.

Section 2 describes the experimental set-up that was developed to measure contact angles from atmospheric pressure to 141 bar. Furthermore the sample preparation and experimental procedure are described. This section also describes the image processing procedure to remove artefacts and to enhance the droplet contour line. Section 3 discusses the contact angle measurements in terms of the wetting behavior of the coal. We end with the conclusions.

2 Experimental

2.1 Experimental set-up

The experiments were carried out in a pendant drop (PD) cell [13] adapted to perform captive bubble contact angle measurements. The cell itself is a stainless steel tube with a void volume of approximately $16cm^3$. Thermally pre-stressed glasses serve as looking glasses at both ends of the cell. Viton O-rings seal between the glasses and the cell. Through the backside, light is provided; the front side is connected to an endoscope and a digital camera with a pixel resolution of 640×400. The cell can withstand pressures up to 600 bar at temperatures up to 200^oC. This is well within the limit of the conditions of interest to us i.e. pressures ranging from 1 bar to 141 bar and a temperature of 45^oC. The cell is built in an insulated air cabinet that provides stable temperatures ($\pm 0.2^oC$). The cell is connected to a single working piston high-pressure displacement pump. This pump enables water injection into the cell and is used to obtain the desired experimental pressure within the system. A capillary tube is connected at the bottom of the cell and serves as a gas injection device. At the end of the capillary, an exchangeable tip with an outer diameter of $1.59mm$ is mounted. The tip can be recognized at the lower part of the images. The capillary is connected to a micro-needle valve and a high-pressure gas reservoir. The needle valve restricts the amount of gas transferred from the reservoir to the injection part to control the droplet volume at the end of the tip.

2.2 Sample preparation

The coal sample used for the experiments was mined in England. Several coal samples were drilled from a lump of coal and cut into a small blocks of a few centimeters length using a diamond saw. One side was polished according to a methodology given elsewhere [3]. Firstly, the coal sample was wet polished with a series of abrasive papers with a grit from 60 to 1200. This was followed by polishing with $0.5\mu m$ abrasive alumina powder and a fibrous cloth. Water

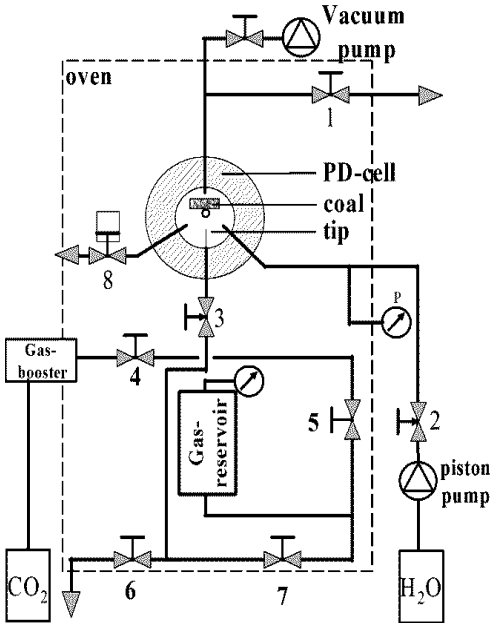

Figure 1: Schematic view of the set up.

washing and ultrasonic cleaning finalized each polishing step. The sample was stored under vacuum and submersed in doubly distilled water for $48h$. This procedure allowed the removal of air from the coal pores and water to penetrate the pore system. The coal sample was built in the sample holder and transferred to the experimental set-up.

All measurements were performed on an anthracitic coal sample. Ultimate and proximate analysis results are given in Table 1. A more homogeneous pore size distribution and chemical composition can be expected in an anthracitic coal sample than for coals of low and medium ranks.

Table 1: Results of the coal petrology, proximate (PA) and ultimate (UA) analysis

PA		UA	[%]	petrology	[%]
moisture [%]	1.3	Carbon	85.68	R_{max}	2.41
Volatile matter (w.f.) [%]	10.4	Hydrogen	3.36	Vitrinite	73.6
Ash (w.f.) [%]	3.9	Nitrogen	1.56	Liptinite	0
Fixed carbon (d.a.f.) [%]	89.3	Sulphur	0.68	Inertinite	24.6
Calorific value [MJ/m^3]	33.2	Oxygen	5.58	Minerals	1.8

2.3 Experimental procedure

First the PD-cell (see Fig. 1) with the coal sample built in is evacuated while valves 1, 2, and 3 are closed. Then, with the vacuum pump still running, valve 2 is opened and deaerated water is slowly injected into the cell. When the cell is completely filled with water, the vacuum pump is switched off. At this point the cell contains water at atmospheric pressure. Valve 1 is opened and water at atmospheric pressure is circulated for eight hours to clean the cell and tubing. A Du-Nouy ring measures the surface tension of the injected and produced water which both attained values of $0.054\ \mathrm{N}/\mathrm{m}$. Carbon dioxide was flushed via valves 4, 5, 7, and 6 to avoid air contamination in the experiment. If a higher pressure than atmospheric is required, the piston pump is used to increase the water pressure in the cell. Subsequently, the gas reservoir is filled with carbon dioxide via the gas booster and valves 4 and 5 until the pressure exceeds the water pressure in the cell by 10 bar. Finally all valves are closed and the system is allowed to reach thermal equilibrium for 48 hours before it is ready to use. In order to simulate reservoir conditions the set-up was kept at a constant temperature of 45^o.

For experiments at atmospheric pressure valve 1 remains open. For high pressure experiments this valve is closed. In order to inject small portions of gas, valve 7 is opened and subsequently closed to fill the small volume between valves 3, 6, and 7 with carbon dioxide. Needle valve 3 is opened to allow small amounts of gas to enter the PD-cell. After some time the carbon dioxide becomes visible as a droplet at the end of the tip. The droplet grows until it hits the coal surface. Gas injection is stopped by closing valve 3. The droplet gradually decreases its size. During this process a camera, connected to an endoscope, captures images of the droplet until the droplet completely disappears.

A Matlab routine was programmed to convert the images into black and white, followed up by an edge enhancement procedure and finally cropped by a selected set of coordinates. Then the cropped images were subjected to a procedure to determine the contact angles. The procedure is fairly simple with just a few parameters that need to be adjusted. The parameters are chosen such that (1) the white ring due to refraction in the middle part of the droplet is discarded, (2) distorted points (due to the shadow of the droplet on the coal surface) are removed, (3) five adjacent points at the coal water interface at the leftmost part of the image are connected with five adjacent points at the rightmost part to find the base line. For the upper left part in the image the X- and Y-coordinates of the white pixels are used to calculate the mean coordinates of the left-side curve representing the water-CO_2 interface and also the slope and direction. The same is done for the upper right part. With these mean coordinates and the slopes, the angles can be calculated with respect to the base line (see Fig. 2).

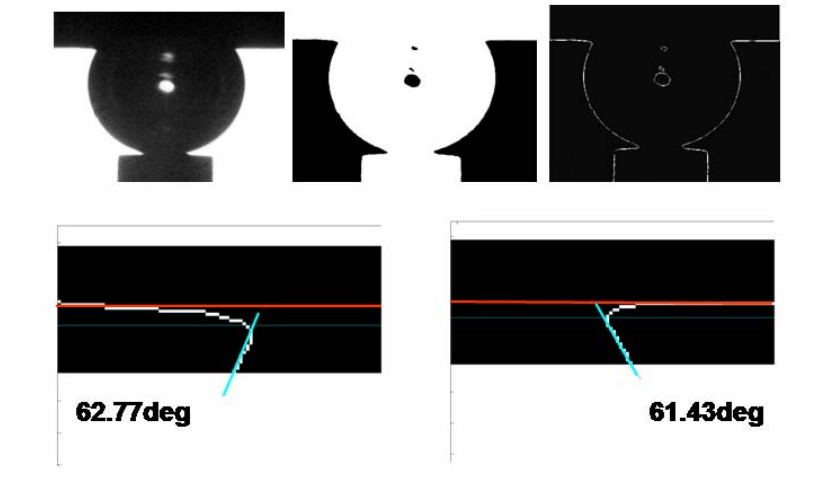

Figure 2: Image processing of droplet and determination of left and right contact angles. The top left shows the raw image. The top middle shows the same droplet converted to a black and white image. The right top droplet shows the result of the edge enhancement. Below the magnified image near the three phase contact line to determine the contact angles.

2.4 Experimental results

Experiments have been performed at various pressures between atmospheric and 141 bar. At atmospheric pressure the following sequence of events is observed (see also Fig. 3). The gas pressure is slightly increased until CO_2 forms a droplet at the top of the tip. The droplet increases to a size of about $2mm$ diameter and is captured between the tip and the coal surface. The contact angle is about 66^o. The droplet size decreases and the contact angle increases up to 77^o. The pressure remains constant, but still small amounts of CO_2 are released by the tip. This CO_2 merges with the droplet, which consequently increases its size and the contact angle again decreases. During the first 190 minutes occasional releases of CO_2 occur and the droplet size fluctuates accordingly. Then the CO_2 supply stops, the droplet size decreases and the contact angle gets back to 62^o. The droplet size steadily decreases. As the droplet reaches a critical volume at 300 minutes it is released from the tip and is only captured by the coal surface above. Subsequently its size decreases until it disappears after three hours and forty minutes, but the contact angle increases slightly and fluctuates around 84^o. The droplet shape is almost spherical throughout the experiment. Contact

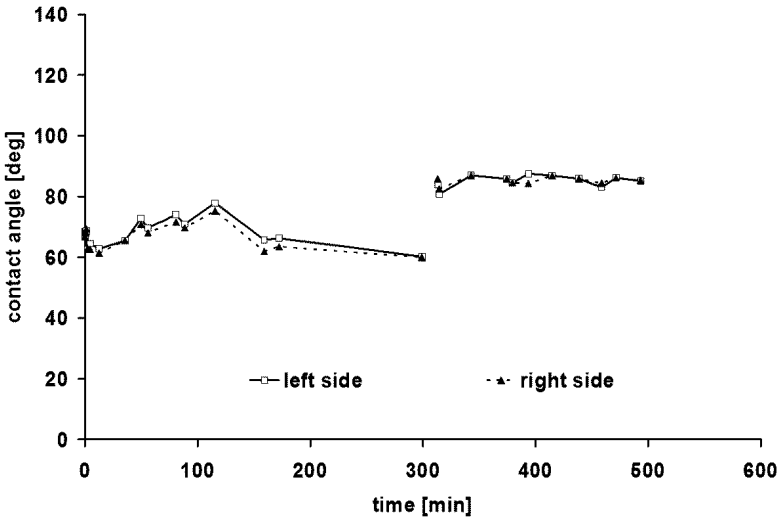

Figure 3: Contact angle history for the atmospheric experiment. Left and right contact angles are indicated. At the discontinuity the droplet is detached from the tip.

angles can be measured until the diameter of the droplet drops below $0.3mm$. The same small disappearance rate is observed when a glass plate covers the coal surface.

At higher pressures (> 2.6 bar) the same procedure is used as for the atmospheric experiments. The same sequence of events occur when the droplet size fluctuates due to occasional releases of CO_2 from the tip. In this period, however, the droplet shows an overall trend of decreasing in size much faster than in the atmospheric experiment. Also after detachment from the tip, the droplet decreases in size much faster than for the atmospheric experiment e.g. for the 2.6 bar experiment the droplet completely disappears in about an hour. After detachment the droplet is no longer shperical and starts to spread on the coal surface.

For the high pressure (> 2.6 bar) experiments the droplet, after its release from the tip, disappears in 20 ± 8 minutes. A plot of the disappearance rate versus the pressure shows, in spite of large scatter, a trend inversely proportional to the square root of the pressure. A typical example of the sequence of events in such a high pressure (96 bar) experiment is shown in Fig. 4.

At $t = 0$ the droplet just touches the coal surface, but is still attached to the tip. A contact angle of about 50^o is observed. As time progresses, the contact angle steadily increases as the droplet size decreases. After three minutes the droplet is detached from the tip. The initial contact angle is about 75^o and increases in a time span of 6 minutes to 120^o. The droplet decreases in size

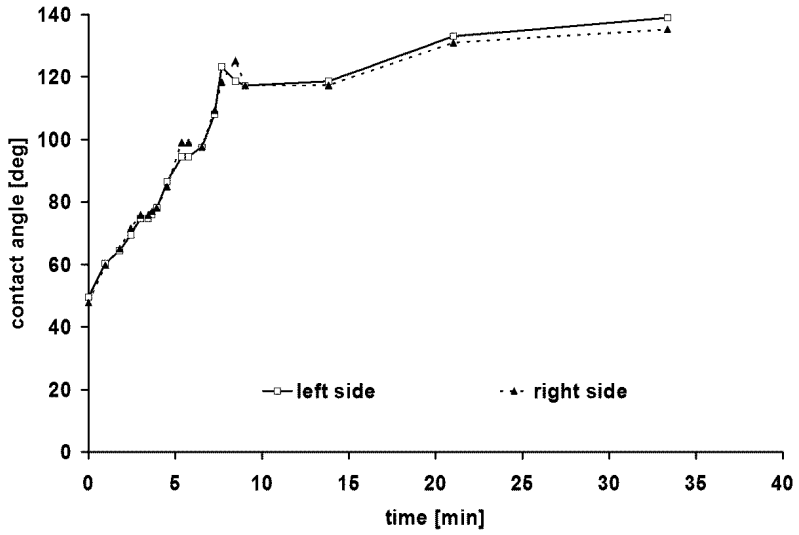

Figure 4: Contact angle history at 96 bar.

during the next 25 minutes until it completely disappears.

In all experiments the following behavior is observed. When the droplet is released from the tip, it finds several optimal positions in time, depending on the droplet size. It is therefore always slightly shifted from a position vertically above the tip. The difference between the right and left contact angle is always less than 10^o and usually less than 5^o. Also in all experiments, the disappearance rate is about the same when the coal surface is covered with a glass plate.

Fig. 5 shows the contact angles for all 15 experiments at the start (solid triangle) and the end of the experiment (open square). At the start of the experiments the droplet is still attached to the tip and contact angles below 90^o are observed. In all experiments with $P > 2.6$ bar, contact angles larger 90^o are observed some ten minutes after the droplet is released. Fig. 5 shows these average (between left and right) contact angles just before the droplet becomes too small to be measured. Only for the atmospheric experiment the contact angle remains below 90^o. A least squares analysis using the data for contact angles, observed at the end of each experiment, was carried out. The slope for the large contact angles for 95% confidence limits (two times the standard deviation) is 0.17 ± 0.14 [deg/bar] i.e. a significant increase of the contact angle with pressure. We excluded the atmospheric pressure point in the least squares analysis. The intercept (the contact angle for $P = 0$) is $111^o \pm 10.5^o$ also for 95% confidence limits. The standard deviation for the contact angles with respect to these lines is somewhat below 15^o. Contact angles observed in Figure 5 at the start of the experiment (solid triangles) do not show a significant trend with pressure.

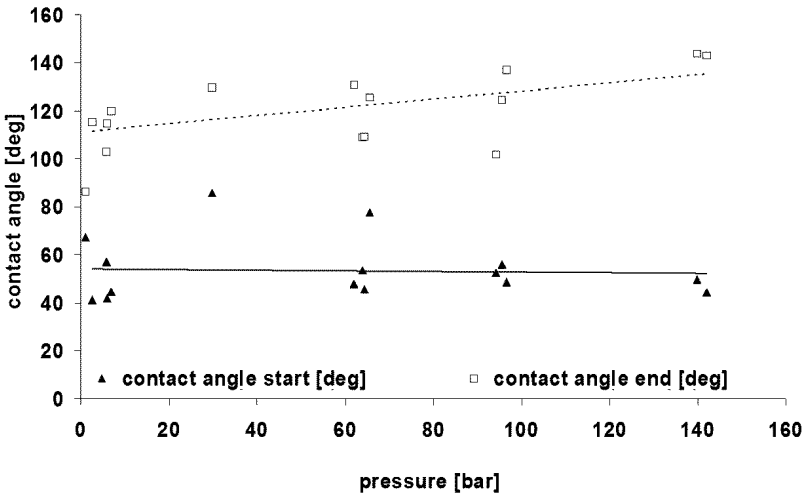

Figure 5: Contact angles at start and end of the experiments as a function of pressure. Contact angles at the start are all below 90^o. Contact angles at the end of the experiment exceed 90^o, except for the experiment performed at atmospheric pressure.

3 Discussion

The reason for the slow disappearance rate of the droplet at atmospheric pressure is not clear. Given the fact that the CO_2 concentration in the gas phase ($0.04 mole/l$) and the concentration in the liquid phase ($0.034 mole/l$) at P=1 bar) are similar we expect that the characteristic disappearance time τ for a droplet with a radius R of $1mm$ is in the order of $R^2/D = 10^{-6}/2 \times 10^{-9} = 500$ seconds, independent of pressure. This characteristic time is indeed observed for the higher pressure experiments, but at atmospheric pressure the droplet survives much longer (see Fig. 3). As the same slow dissolution of the droplet is observed when the coal surface is covered with a glass plate, we conclude that the droplet mainly disappears due to dissolution in the water phase and not due to adsorption on the coal. We also observe that the atmospheric experiments shows different behavior from all the other experiments (e.g. Fig. 4) as to the contact angle.

The contact angle behavior can be qualitatively understood as follows. When the droplet is captured at the surface a local water film exists between the CO_2 droplet and the coal surface. Hence the surface appears to be initially water-wet. As time proceeds the water film thins because of drainage and evaporation until the film is ruptured. Therefore the CO_2 droplet is bounded above by a surface that consists of water free coal and patches of water films on the surface. The number of water film patches decreases as time proceeds. Keller [15] found that

the cosine of the observed contact angle is an average of the cosines of the contact angles between carbon dioxide and the heterogeneous coal surface, including patches of water films. The three phase contact line cannot follow the local contact angle behavior on a heterogeneous surface as this would imply a highly irregular water-CO_2 surface with a high surface energy. Therefore it can be expected that the contact angle varies more smoothly and that the left and right contact angle usually differ less than 5^o. It can also be expected that the droplet finds an energetically optimal position that changes with time as the droplet gradually dissolves. As the coal surface consists of hydrophilic mineral parts, initially water filled pores, hydrophobic aliphatic parts and intermediate wet aromatic parts we expect that the coal surface is on average neither totally water wet nor totally carbon dioxide wet. The observation of a decreasing (increasing) contact angle as the droplet size increases (decreases) can be expected from contact angle hysteresis. After the droplet is detached from the tip its size decreases and the droplet is bounded from above by coal that has been exposed to CO_2 from which the water film has partly disappeared. Consequently the contact angle increases. For the atmospheric experiment the increase is small and remains below 85^o. A Comparison to air-water-coal contact angles shows that this value is somewhat higher than computed with the parachor method [16], where for the coal sample used in the experiment values of about 60^o have been found. For the high pressure experiments the contact angle increases to $111^o \pm 10.5^o + (0.17 \pm 0.14)\ P$ [bar] .

It is unlikely that the interaction of CO_2 with the coal surface at atmospheric pressure and at 2.6 bar is completely different. One explanation is that contact angle hysteresis effects are more pronounced for the experiments where the droplet size decreases more rapidly. Another explanation is that water films at the coal surface remain more stable for the same reason that the dissolution rate for the atmospheric droplet is low. For practical purposes we conclude that for the coal used in these experiments the surface is carbon dioxide wet at pressures relevant for carbon dioxide storage in coal layers. Possibly this coal surface is also carbon dioxide wet at atmospheric pressure, but for the duration of the experiment water films prevent the exposure of the coal surface to carbon dioxide. Other coals may show different behavior depending on the mineral/ aliphatic/ aromatic surface composition.

4 Conclusions

- Reproducible contact angles were measured in a water-CO_2-coal system for pressures ranging between atmospheric and 141 bar.
- When the droplet is just released from the tip, the observed contact angles are below 90^o, showing that the system behaves initially water-wet independent of pressure. This can be possibly attributed to the stability of water films remaining on the coal surface.
- At atmospheric pressure the coal remains water-wet with contact angles

θ of 85^o. Above 2.6 bar the contact angle increases with pressure i.e. $\theta = (111^o \pm 10.5^o) \pm (0.17 \pm 0.14)\ P$ [bar], where the errors represent 95% confidence limits. This shows that our coal sample behaves CO_2-wet at pressures above 2.6 bar.

- It is unlikely that the different behavior of the atmospheric experiment with the higher pressure experiments starting at 2.6 bar is due to a difference in interaction energy between the coal surface and the gas molecules. It is more plausible that this behavior is related to the difference in stability of the water film between the coal and the CO_2.

- Indeed, at atmospheric pressures the captured CO_2 droplet dissolves in the water in a time span of several hours. At higher pressures (> 2.6 bar) the dissolution process takes place in several tens of minutes. This may suggest that the same mechanism causes the stability of the water film (low contact angles) and the slow dissolution rate of the droplet at atmospheric pressure.

- Accepting this explanation for the different behavior of the atmospheric experiment we conclude that for this coal sample the water-CO_2-coal system is CO_2 wet at all pressures and becomes only slightly more CO_2-wet at higher pressures. Only due to the slow disappearance of the water film this coal appears to be water-wet at atmospheric pressure.

5 Acknowledgements

The research reported in this paper was carried out as part of the project ICBM-NNE5-1999-20174 under the ENERGY and SUSTAINABLE DEVELOPMENT PROGRAM founded by the European Community. The finacial support is gratefully acknowledged. We thank G.J.M Koper for helpful discussions. We thank B.T. de Haas for reading the final manuscript.

References

[1] A.W. Adamson, A.P. Gast, *Physical Chemistry of Surfaces*, John-Wiley, New York 1997

[2] R.B. Bird, W.E. Stewart, E.N. Lightfoot, *Transport phenomena* John-Wiley New York 1960

[3] J. Drelich, J.S. Laskowski, M. Pawlik,S. Veeramasuneni, J. Adhesion Sci. Technol. **11** (1997) 1399

[4] H.W. Fox, W.A. Zisman, J. Coll. Sci. **5** (1950) 514.

[5] D.W. Fuerstenau, *Office of Surface Mining and Reclamation Enforcement*, U.S. Dept. Interior, final report g/79-12/81.

[6] P.G. de Gennes, Rev. Mod. Phys. **57,** 3 part I (1985) 827.

[7] P.D. Gamson, B.B. Beamish, D.P. Johnson, Fuel, **72** (1993) 87.

[8] J.A. Gutierrez-Rodriguez, R.J. PurcellF.F.Aplan, CoIloids Surfaces **12** (1984) 1.

[9] J.A. Gutierrez-Rodriguez, F.F. Aplan, Colloids Surfaces, **12** (1984) 27.

[10] G.J. Hirasaki, in: N.R.Morrow, (Ed.), *Interfacial Phenomena in Petroleum Recovery,* Dekker, New York, 1991, pp. 23-76.

[11] G.J. Hirasaki, in: N.R.Morrow, (Ed.), *Interfacial Phenomena in Petroleum Recovery,* Dekker, New York, 1991, pp. 77.

[12] G.J. Hirasaki, Society of Petroleum Engineers, SPE 17367.

[13] R. J. M. Huijgens, *The Influence of Interfacial Tension on Nitrogen Flooding,* PhD dissertation, Delft University of Technology (1990).

[14] J.F. Joanny, P.G. de Gennes, J. Chem. Phys. **81** (1984) 552.

[15] D.V. Keller, Colloids and Surfaces, **22** (1987) 21.

[16] D.W. van Krevelen, *Coal, Typology-Physics-Chemistry-Constitution,* Elsevier, Amsterdam, (1993) 493-507.

[17] T. Murata, Fuel, **60** (1981) 744.

[18] J. Spelt, E.L Vargha-Butler in: A.W. Neumann, J.K. Spelt (Eds.), Surfactant science series 63, (1996), p 394.